ELSEVIER

1 October 2002

Optics Communications 211 (2002) 215–223

OPTICS COMMUNICATIONS

www.elsevier.com/locate/optcom

Optical constants of silicon and silicon dioxide using soft X-ray reflectance measurements

Pragya Tripathi, G.S. Lodha *, M.H. Modi, A.K. Sinha, K.J.S. Sawhney, R.V. Nandedkar

Synchrotron Utilisation Section, Centre for Advanced Technology, Indore 452013, India

Received 18 June 2002; received in revised form 14 August 2002; accepted 16 August 2002

Abstract

Using the synchrotron radiation source Indus-1, we have performed the angle dependent reflectance measurements in the soft X-ray region, on etched silicon (1 1 1) wafer and silicon dioxide wafer. The data so obtained is used to evaluate the optical constants 'δ' and 'β' in the wavelength region 80–200 Å for the two materials. The results are compared with the tabulated data of Henke et al. and other reported experimental results. It has been found that the data for silicon is in close agreement with the tabulated data away from the silicon L absorption edge with significant deviations near the edge. The experimentally obtained β values for silicon dioxide are consistent with the Henke's tabulated data where as the δ values show an upward trend with a shift of 9% from the tabulated values.The experimental data is also compared with energy dependent measurements done by Filatova et al. on non crystalline silicon dioxide and it is found that our data although match closely with that of Filatova's below 140 Å, but after 140 Å, Filatova's values for δ show a downward trend while our data follow the same upward trend as the tabulated values of Henke et al.
© 2002 Elsevier Science B.V. All rights reserved.

PACS: 78.20.Ci; 78.20.−e

Keywords: Optical constants; Soft X-ray; Complex dielectric constants; Reflection; Synchrotron radiation; Silicon dioxide; Silicon

1. Introduction

Optical properties of a given material in extreme ultra violet (EUV)/soft X-ray region are described by the optical constants – the real and imaginary parts of the complex refractive index $n = 1 - \delta + i\beta$ [1]. Optical constants of materials in this region of the electro magnetic spectrum are of interest to several areas of technology such as synchrotron radiation applications, X-ray astronomy, and plasma physics etc. However, there are little or no experimentally measured optical constant data available near the region of anomalous

* Corresponding author. Tel.: +91-731-488-002; fax: +91-731-488-000.
E-mail address: lodha@cat.ernet.in (G.S. Lodha).

0030-4018/02/$ - see front matter © 2002 Elsevier Science B.V. All rights reserved.
PII: S0030-4018(02)01950-8

dispersion for most of the elements. Current tabulations of Henke et al. [2] rely largely on transmittance measurements and theoretical calculations, where the real part of refractive index has been calculated using Kramer's–Kronig analysis [3]. Henke et al. tabulations are generally valid away from the absorption edges.

Silicon and silicon dioxide (SiO_2) are the preferred substrate materials for X-ray optical elements and have been extensively used in fabrication of EUV/ soft X-ray multilayer optics [4,5]. Because of the technological importance in semiconductor industry, many studies have been carried out on Si–SiO_2 interfaces [6]. In light of these applications, measurements of the optical response of these materials near the edges are important due to poor reliability of tabulated values. Measurements of the refractive index of silicon and silicon dioxide, around the silicon $L_{2,3}$ edge (124.5 Å) have been reported using various methods [5,7–12] with discrepancies from the tabulated values of Henke et al. [2]. The discrepancies are usually attributed to surface contaminations and inherent difficulties in method of measurements.

In the present study, optical constants of etched silicon wafer and pure silicon dioxide wafer are evaluated using angle dependent reflectance experiments in the region around $L_{2,3}$ edge of silicon. These measurements are performed on Indus-1 synchrotron source using EUV/ soft X-ray reflectivity beam-line. The structure of solid, contamination, oxidation, and phases present, all strongly influence the optical properties near the absorption edge [1]. Angle dependent reflectance measurements have the advantage over transmittance or reflectivity measurements coupled with Kramer's–Kronig analysis, that both 'δ' and 'β' can be deduced experimentally at each energy by fitting the reflected profile. The added advantage of this method being, that the measurements can be performed on the bulk samples and hence there is no need for fabrication of free standing thin films. But this method is highly sensitive to external surface contamination. In the present study, the surface roughness is determined independently using hard X-ray reflectance measurements, and cleaning the sample in ultra violet atmosphere significantly reduced the surface contamination. The experimental data obtained by us is compared with the measurements of Soufli and Gullikson [5] for silicon sample and with the measurements of Filatova et al. [10–12] for silicon dioxide.

2. Basic principle

An electromagnetic plane wave $E = E_0 \exp[-i(\omega t - kr)]$, propagates in medium of refractive index n according to Helmoltz equation [13]

$$\Delta E + k^2 n E = 0,$$

where $k = (2\pi/\lambda)$, modulus of wave vector $\mathbf{k}$, λ denotes the X-ray wavelength.

For photon energies above 30 eV the scattering of radiation is mainly with individual atoms rather than condense state of the system. In this case total scattering amplitude is vector sum of the amplitudes scattered by the individual atoms. The optical properties of material can be described by the atomic scattering factor. The index of refraction of material is related to scattering factor by [1]

$$n = 1 - \delta + i\beta = 1 - \frac{r_e}{2\pi}\lambda^2 N_a f,$$

where δ and β are optical constants, δ is called refractive index decrement and β is absorption index. N_a is atomic density, r_e is classical electron radius, and f is atomic scattering factor. In general the atomic scattering factor depends both on scattering angle and wavelength. However, for long wavelengths and/or small scattering angles, the scattering factor becomes independent of scattering angle. The complex atomic scattering factor equals to forward scattering factor $f(\theta = 0)$

$$f = f(\omega) = f_1(\omega) - i f_2(\omega).$$

The real and imaginary parts f_1 and f_2 of scattering factor are related to optical constants δ and β [1]

$$\delta \cong \frac{r_e}{2\pi}\lambda^2 N_a f_1,$$

$$\beta \cong \frac{r_e}{2\pi}\lambda^2 N_a f_2.$$

The absorption term f_2 can be determined experimentally over the broad energy spectrum by transmission measurements of freestanding films

of materials. With given knowledge of one of scattering parameters, the other can be calculated by an integral transform using Kramer's–Kronig relation [13]

$$f_1(\omega) - Z = -\frac{2}{\pi}\int_0^\infty \frac{\omega' f_2(\omega')}{\omega'^2 - \omega^2}\,\mathrm{d}\omega'.$$

In the high photon energy limit, f_1 approaches Z, the number of electrons in atom contributing to absorption. In general the calculation of optical parameters using this integral involves difficulties, mostly due to the absorption/reflection measurements over a limited frequency spectrum, whereas the integral requires the knowledge of f_2 over whole frequency spectrum. Furthermore, one needs extremely thin contamination-free free-standing foils. Outside the spectral range of experiment the extrapolations are used, adding uncertainties in calculations.

The angular dependency of reflection by means of Fresnel's formulae provides another way to obtain optical constants. For s-polarized light the Fresnel's reflection coefficient can be written as [13]

$$r_s = \frac{\sin\theta - \sqrt{n^2 - \cos^2\theta}}{\sin\theta + \sqrt{n^2 - \cos^2\theta}}.$$

Here θ is grazing angle of incidence with respect to the sample surface. In this case the reflection spectra at discrete photon energy are obtained. By this means both δ and β can be obtained simultaneously. This method is sensitive to surface contaminations and morphological rms roughness. The later can be taken into account as per Nevot–Croce model [14]. The shape of the reflection spectra is sensitive to β/δ ratio. The ratio significantly affects the calculations of optical constants near the absorption edges [5].

3. Experimental

3.1. Sample preparation

The samples used in this experiment are (i) (1 1 1) oriented polished n-type silicon wafers and (2) chemical vapor deposition grown silicon dioxide wafer which is exceptionally smooth and has a density of fused silica ($\sim$2.2 gm/cm^3). Prior to reflectance measurements the samples are cleaned. The inherent contamination on the sample is removed using a process very similar to that used in the removal of organic and hydroxyl impurities of silicon wafer and synchrotron optics elements [15,16]. The process consists of heating the sample in a quartz tube in an oxygen rich environment at a temperature of 200 °C for about 16 h. It is simultaneously irradiated by an ultra violet (UV) mercury discharge lamp. The UV rays from lamp have two bands, one at 1849 Å and other at 2537 Å, which are found to be important in cleaning. The 1849 Å light dissociates oxygen (O_2) and produces ozone (O_3). The 2537 Å light initiates photodecomposition of ozone into O_2 and an activated 'O' atom, which reacts with the hydrocarbons on the sample surface and decomposes them into volatile compounds such as H_2O and CO_2 [15]. The 2537 Å light is also believed to photosensitize organic contamination and hence result in enhanced cleaning rates. There is a strong concentration gradient of ozone near the UV lamp because of the fact that 1849 Å light has a low penetration depth in air and 2537 Å light has a long penetration depth. Thus the cleaning rates are strongly dependent on the lamp distance from the sample. The sample has to be near the lamp for effective cleaning. We have used a distance of 1.5 cm. The activated 'O' atom at the same time oxidizes the sample surface also. However, this effect is not a problem for silicon dioxide as it is already an oxide material. For silicon wafer, after this cleaning procedure the sample is etched in a mixture of hydrofluoric acid and ethanol, in the ratio of 1:10 for 5 min. The sample is then rinsed in ethanol and dried in pure nitrogen environment. This procedure passivates the dangling bonds on the silicon surface by hydrogen atoms (H-passivation).

Immediately after cleaning the sample, it is mounted in the reflectometer chamber and is kept in clean high vacuum. Photoelectron spectroscopy (PES) studies on different samples cleaned by this procedure was done earlier and it is found that the total surface impurities reduce considerably. Fig. 1 shows the PES results on cleaned and etched silicon samples. PES analysis is performed using Al K_α (8.34 Å) source on Si wafer before and after

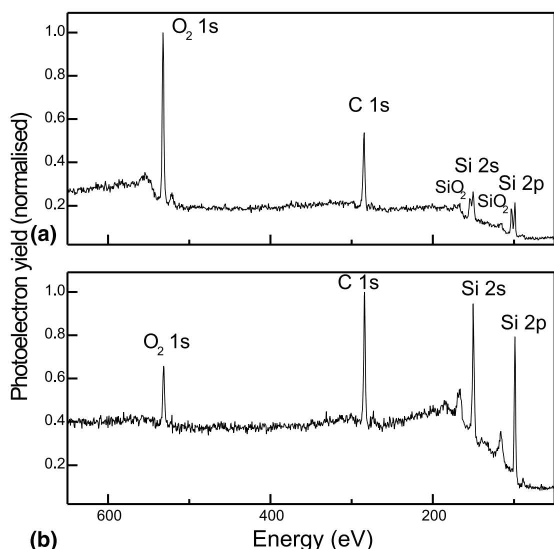

Fig. 1. PES spectra of (a) untreated Si(1 1 1) wafer, a high carbon (284.6 eV) and oxygen (532.28 eV) contamination peaks are seen. (b) UV irradiated and etched Si(1 1 1) wafer, the silicon peaks are much larger than the 'C' and 'O' peaks now.

H-passivation. In a commercially available silicon wafer, the PES data showed, Fig. 1(a), a very high oxygen (1s peak at 532.28 eV) and carbon (1s peak at 284.6 eV) contamination on the surface. Also the silicon dioxide peaks (at 154.68 and 103.48 eV) are clearly seen with the silicon 2s and 2p peaks (150.2 and 99 eV, respectively) and the intensity are comparable to that of silicon peaks. After UV treatment and HF etching it is found that, Fig. 1(b), the oxygen contamination is reduced by 80% and carbon by 50% of that before cleaning. The silicon dioxide peaks disappeared completely.

3.2. Reflectance measurements

The angle dependent reflectance measurements on the etched silicon wafer and pure silicon dioxide wafer has been carried out on the Indus-1 synchrotron source (450 MeV storage ring, critical wavelength, $\lambda_c \sim 61$ Å) [17], in the soft X-ray regime (80–200 Å). Indus-1, is the first synchrotron facility in India commissioned recently. The reported studies are first few studies on the source. The polished Si wafer and SiO_2 wafer used are well characterized beforehand by hard X-ray reflectance and microscopy [4] for it's surface quality. The rms roughness of polished unetched silicon wafer is 7 Å and SiO_2 wafer is 6 Å as determined from hard X-ray reflectance measurements. Etching/cleaning process increases the roughness of silicon wafer sample to 10 Å for our etched-1 sample and 13 Å for our etched-2 sample. The reflectance measurements are carried out on the bending magnet reflectometry beam-line on Indus-1 source. The beam-line provides monochromatic photons in 40–1000 Å wavelength region with a moderate spectral resolution and high intensity, using a torroidal grating monochromator [17]. In the present measurements, in the wavelength range of 80–200 Å, the wavelength resolution ($\lambda/\Delta\lambda$) is 200–300. The higher diffraction order contamination is removed by inserting various absorption edge thin film filters. The experimental chamber consists of two rotary stages driven by stepper motors and a linear translation stage for sample mounting.Stepper motors are used in micro stepping mode to obtain an angular resolution of 0.0025°. The detector used is EUV/ soft X-ray photodiode, its signal being measured using pico ampere current amplifiers. High vacuum (10^{-8} mbar) is maintained in the reflectometer chamber.

The θ–2θ scan is performed, in the s-polarized geometry, on both the samples, at different wavelengths in the range 80–200 Å. The reflected photodiode current is normalized to the incident intensity. The main source of instrumental error is the electronic noise in the photodiode current. This error was less than 0.3% at the lowest reflectance value measured. The angular reflectance scan at a particular wavelength is from 0–50°. Experimental data so obtained is used in the determination of the optical constants.

The specular reflectance curves $R(\theta)$ are fitted using Fresnel's equations for an infinitely thick material. A non-linear least squares curve fitting technique based on the χ^2 minimization is applied for the derivation of optical constants from reflectance measurements [9]. The fitting is performed over the angular range of 2–50°. The model for fitting the reflectance depends upon the quantities δ and β for the material(s), the substrate and interface(s) roughness σ's, and incident angle (θ). 'θ' is taken as an independent variable. To reduce the number of adjustable parameters, rms

roughness is assumed for each sample depending upon the hard X-ray reflectance and atomic force microscopy results [4]. The choice of keeping 'σ' fixed was made after observing the sensitivity of the fitting algorithm to only two adjustable parameters (δ and β). The effect of rms roughness ($\leqslant 4$ Å) modified the fitted values of δ and β by less than 0.2%. Optical constants remained the variable parameters in the curve-fitting algorithm. For clean surfaces a single layer model is fitted with two variables, and for contaminated surfaces a two-layer model is fitted with four variables (two set of δ and β). Optical data available in the literature is used as an initial guess for the δ and β of materials. Separate calculations and corrections are made for different samples, according to the surface analysis results for the top layer thickness.

4. Results and discussion

4.1. Silicon wafer

Fig. 2 shows the reflectance curves along with the best-fit profiles, for the hydrogen passivated silicon wafer sample (etched-1) at different wavelengths. Theoretically, after H-passivation, the silicon wafer surface should be stable against any new oxidation. However, the cleaning is not 100% effective (as seen in our PES results), and there are always some dangling bonds or oxidation sites that initiates a slow degradation of the surface. In general the cleaning results highly depend on the amount of organic substance in the atmosphere and also on other undetermined factors such as recontamination from vessels and handling. Even after cleaning and H-passivation, an ultra thin SiO_2 layer is present. By fitting the reflectivity far from the absorption edge of silicon, we derived a 15 Å thick layer of SiO_2 on the top surface and a surface roughness of 10 Å. The top layer thickness and roughness are fixed parameters for the non linear least square fitting of data at all the other wavelengths.

The same experiment is repeated with an untreated silicon wafer sample and another etched sample (etched-2). Fig. 3 shows the reflectance curves for the three samples at $\lambda = 135$ Å. In fitting

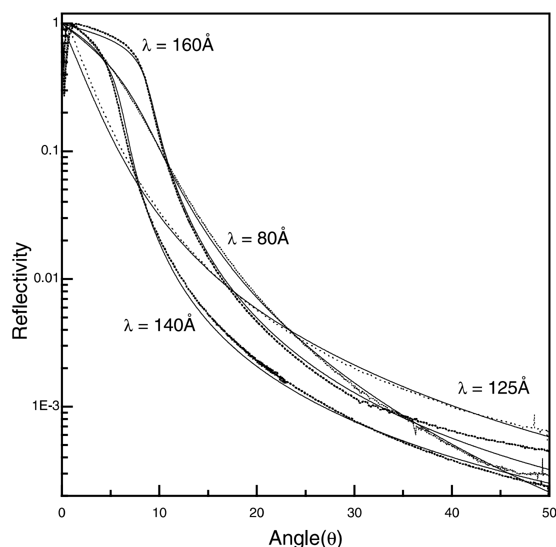

Fig. 2. Angle dependent reflectance curves (dotted lines) at wavelengths $\lambda = 80$, 125, 140 and 160 Å, along with the best-fit profiles (continuous lines), for UV irradiated and etched silicon sample (etched-I). A roughness of 10 Å and a top SiO_2 layer thickness of 15 Å are used for fitting.

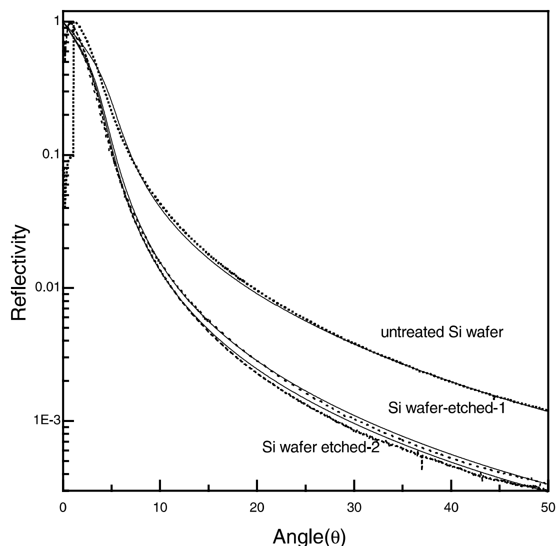

Fig. 3. Angle dependent reflectance curves (dotted lines) at $\lambda = 135$ Å, along with the best fit profiles (continuous lines) for – (i) untreated silicon wafer sample, fitting done by assuming a top SiO_2 layer thickness of 30 Å and roughness 7 Å, (ii) etched-I sample, fitting done by assuming a top layer SiO_2 thickness of 15 Å and a roughness of 10 Å and (iii) etched-II sample, fitting done by assuming a top layer SiO_2 thickness of 15 Å and a roughness of 13 Å.

of the etched-2 sample the δ, β and top layer thickness are the same as etched1 sample, only the roughness parameter is increased to 13 Å. The increase in roughness is accounted by the fact that etching rate is very sensitive to the time the sample is kept in HF/ethanol solution. It is clear from the overlapped region of the etched-1 and etched-2 curves that the choice of β/δ and top layer thickness is correct. A thicker silicon dioxide layer (30 Å) and a lower roughness (7 Å) as measured using hard X-ray reflectance is used for fitting of the untreated sample.

Fig. 4 shows δ and β values obtained by fitting the experimental angle dependent reflectance values over the full angular region, along with the Henke's values [2].The values of δ and β between 130 and 160 Å are in good agreement with the Henke's tabulated values [2] and values from reflectivity and transmission measurements [5]. The variation in δ is within ±3% and in β it is ±5%. From 80 to 120 Å, variation in δ is within ±7% and in β it is ± 9%. These larger deviations at shorter wavelengths are inherent in the reflectance measurement procedure, as absorption is high in this region. At the edge (125 Å) there is a large deviation from the tabulated value, because at the edge the values are highly sensitive to phase composition and to the atomic arrangement, leaving this method not suitable for calculation in that regime.

4.2. Silicon dioxide wafer

Fig. 5 shows the reflectance curves along with the best-fit profiles for SiO_2 wafer for wavelengths 80, 100, 125 and 130 Å. Fig. 6 shows the reflectance curves along with the best-fit profiles for SiO_2 wafer for wavelengths 135, 140, 160 and 200 Å. The fitting of the data has been carried out using a tabulated mass density of 2.2 gm/cm^3 for fused silica and rms roughness of 5 Å obtained from hard X-ray reflectance and atomic force microscopy results [4]. It is reported that, for SiO_2 the presence of water or hydroxyl absorption in the samples makes the determination of the δ and β extremely difficult in certain parts of the vacuum UV/soft X-ray spectral regions [7]. In the present study this difficulty is avoided by the cleaning procedure. No top contamination layer or defects are introduced in the algorithm to fit the data. The optical constants δ and β are the only variable parameters here.

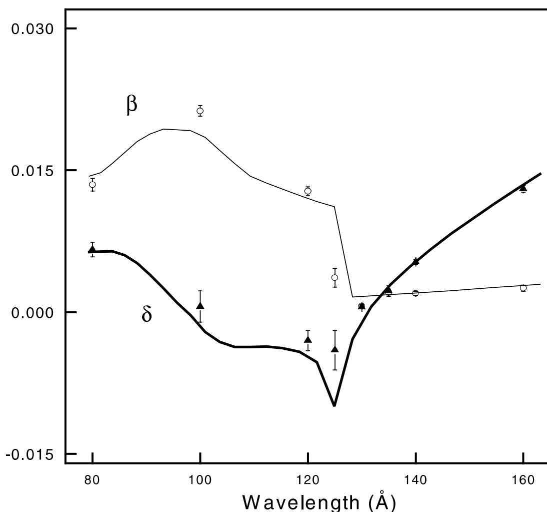

Fig. 4. Optical constants for silicon wafer, experimentally obtained values are plotted along with the Henke's [2] tabulated values (continuous lines — and —). The open circles (○) represent experimental data points for 'β' and the filled triangles (▲) for 'δ'.

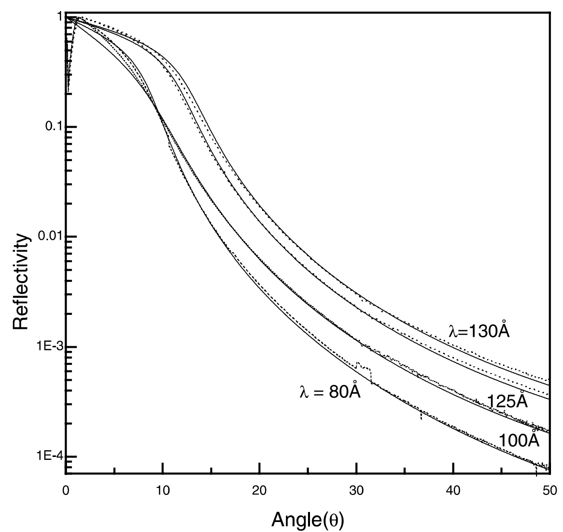

Fig. 5. Angle dependent reflectance curves (dotted lines) along with the best-fit profiles (continuous lines) for SiO_2 wafer sample at $\lambda = 80$, 100, 125 and 130 Å. The fitting is done assuming no top contamination layer, and a roughness of 6 Å.

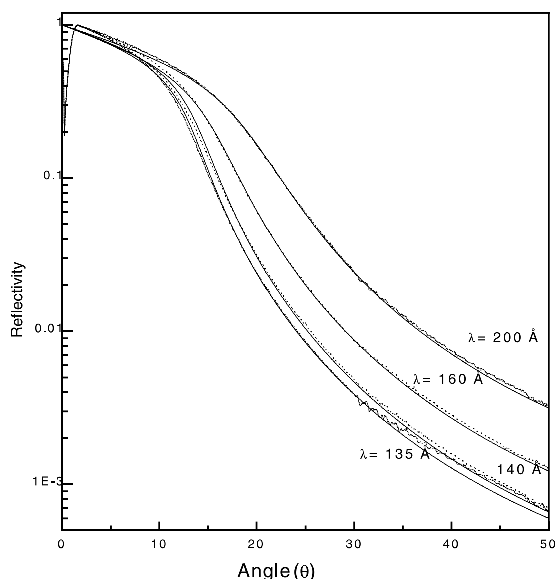

Fig. 6. Angle dependent reflectance curves (dotted lines) along with the best-fit profiles (continuous lines) for SiO_2 wafer sample at $\lambda = 135$, 140, 160 and 200 Å. The fitting is done assuming no top contamination layer, and a roughness of 6 Å.

Filatova et al. [12] have reported the optical constants of SiO_2 in 60–3000 eV photon energy range (wavelength range $\lambda = 4$–200 Å). The sample used by them is 1200 Å thick SiO_2 layer grown on silicon substrate by dry oxidation method at ~1050 °C. They have measured a reflection spectra using synchrotron radiation at a grazing angle of 0.6° in the wavelength range 4–200 Å. This spectral region included Si $L_{2,3}$, O K, Si K absorption edges. The optical constants were then calculated by them using the Kramer's–Kronig analysis in this range. Also, they have tried to examine the problem of calculation of dispersion of optical data using this analysis more closely by using the angle dependent reflectance measurements carried out at some energies.

Table 1 gives the values of δ and β, our experimentally obtained values along with the tabulated (Henke's) values [2] and those obtained by Filatova et al. [12]. The data of Henke et al. has been used to calculate the optical constant for a compound (SiO_2), by assuming the atomic scattering factors of silicon and oxygen in weighted proportion. The optical constants reported by us are by angle dependent reflectance measurements, which have an added advantage that, both δ and β are deduced by fitting the measured reflectance profile. Thus it provides a test of tabulated values of δ generated by Kramer's–Kronig relations. In the present set of calculations, the optical constants, δ and β, are the only variable set of parameters, which are also regarded as independent of each other in this parameter estimation model.

Fig. 7 shows the plot of δ and β versus wavelength. The solid line shows the tabulated values of Henke et al. [2], whereas the scattered points are our experimental values and the dotted line are values obtained by Filatova et al. [12]. It is seen that our experimental values for δ are shifted upwards from the Henke's tabulated data in the

Table 1
Optical constants of SiO_2 wafer

Energy (eV)	λ (Å)	δ(Henke)	δ(expt.)(err)	δ(Filatova)	β(Henke)	β (expt.)(err)	β(Filatova)
155.00	80	0.010606	0.0114(3)	0.01114	0.008105	0.0057(7)	0.00709
124.00	100	0.011920	0.0122(7)	0.01187	0.012046	0.0121(9)	0.01028
103.33	120	0.013517	0.0168(3)	0.01689	0.013567	0.0080(7)	0.00826
99.20	125	0.014661	0.0211(4)	0.02015	0.008936	0.0093(9)	0.00914
95.38	130	0.019129	0.0240(5)	0.02335	0.009781	0.011(1)	0.01076
91.85	135	0.021938	0.0265(4)	0.02448	0.010771	0.011(1)	0.01167
88.57	140	0.024350	0.0287(5)	0.02814	0.011842	0.012(1)	0.01403
77.50	160	0.033759	0.0373(7)	0.03434	0.017042	0.018(1)	0.01848
65.26	190	0.046959	0.0507(9)	0.04207	0.027442	0.027(2)	0.02727
62.00	200	0.051422	0.055(1)	–	0.031373	0.031(2)	–

Our experimental values are compared with the tabulated data by Henke et al. [2], and the experimental data on noncrystalline SiO_2 by energy dependent measurements, by Filatova et al. [11].The fitting errors in our experimental measurements for the last significant digit are given in brackets along with the δ and β values.

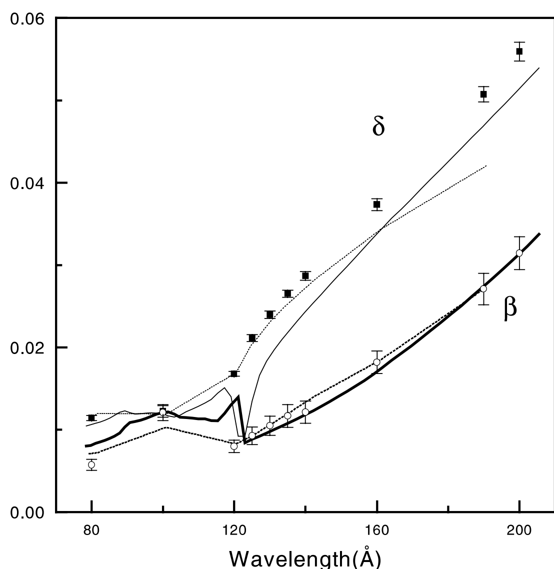

Fig. 7. Optical constants for silicon dioxide sample, experimentally obtained values are plotted along with the Henke's [2] tabulated values and those obtained by energy dependent measurements by Filatova et al. [11]. The filled rectangles (■) represent experimentally obtained δ and open circles (O) β. The continuous lines (— and —) are Henke's values for δ and β. The dotted curves (··· and - - -) are Filatova's values for δ and β.

whole wavelength range (80–200 Å). In the wavelength region 80–140 Å the δ values from our experiment match with those of Filatova et al. within ±4%. The experimental values show an upward shift from the Henke's values by around 15% in this wavelength range. After 140 Å our experimental values follow the same upward trend (15% deviation upwards from tabulated) whereas the values of Filatova et al. decreases from the Henke's values.

5. Conclusions

Angle dependent reflectance measurements have been performed using a reflectometer on a TGM beam line of synchrotron radiation source Indus-1, on super polished silicon wafer and silicon dioxide wafer sample in the wavelength region 80–200 Å. Surface analysis using the PES measurements show that the cleaning procedure consisting of UV irradiation is successful in removing the 'C' contamination, and subsequent etching in case of silicon wafer removes the native oxide layer on it and H-passivated surface is achieved. The measurements are carried out near the silicon $L_{2,3}$ edges in both the cases.

The experimental results on silicon wafer are in close agreement with those that have been reported earlier. It is found that the experimentally obtained optical constants agree within ±7% with the tabulated data of Henke et al. [2] above and below the absorption edge of silicon, whereas at the absorption edge the variation is large. The results are compared with those of Soufli and Gullikson [5], and they agree well.

Optical constants for silicon dioxide are reported in the wavelength range 80–200 Å. The theoretical data obtained by assuming the atomic scattering factors of silicon and oxygen in appropriate mixture, matches closely above the wavelength 125 Å and below 100 Å. The reflectance data obtained by us is also compared with the energy dependent reflectance measurements done by Filatova et al. and the variation between the two is found to be within 4% for δ in the wavelength region 80–140 Å and 9% for β in the wavelength region 124–200 Å. After 160 Å there is a downward fall in the Filatova's values for δ and our experimental data follows the same upward trend as the Henke's data. In between 100 and 125 Å the problem arises due to the presence of silicon absorption edge in between and the dependence of fitting algorithm on β/δ value.

Acknowledgements

The authors acknowledge T. Sripati, IUC, Indore, for the PES measurements. The authors also thank the Indus-1 operation staff for the help during experiments. Our thanks are also due to R.K. Gupta and M.N. Singh for their co-operation in running the beamline.

References

[1] E. Spiller, Soft X-ray Optics, SPIE, Bellingham, WA, USA, 1994.

[2] B.L. Henke, E.M. Gullikson, J.C. Davis, At. Data Nucl. Data Tables 54 (1993).
[3] N.K. Del Grande, P. Lee, J.A. Samson, D.Y. Smith (Eds.), Proc. SPIE, 911 (1988) 86–99.
[4] G.S. Lodha, K. Yamashita, H. Kuneida, Y. Tawara, J. Yu, Y. Namba, J.M. Bennet, Appl. Opt. 37 (1998) 5239.
[5] R. Soufli, E.H. Gullikson, Appl. Opt. 36 (1997) 5499.
[6] C.M. Herzinger, B. Johs, W.A. McGahan, J.A. Woollam, J. Appl. Phys. 83 (1998) 3323.
[7] E.D. Palik (Ed.), Handbook of optical constants of solids, Academic, Orlando, 1998, p. 749.
[8] M. Zukie, D.G. Torr, J.F. Spann, M.R. Torr, Appl. Opt. 29 (1990) 4284.
[9] D.L. Windt, W.C. Cash Jr., M. Scott, P. Arendt, B. Newnam, R. Fisher, A.B. Swartzlander, P.Z. Takacs, J.M. Pinnes, Appl. Opt. 27 (1988) 279.
[10] E.O. Filatova, A.I. Stepanov, V.A. Luk'yanov, Opt. Spectrosc. 81 (1996) 416.
[11] E. Filatova, V. Lukyanov, J. Electron Spectrosc. Relat. Phenom. 79 (1996) 63.
[12] E. Filatova, V. Lukyanov, R. Barchewitz, J.M. Andre, M. Idir, Ph. Stemmler, J. Phys. Condes. Matter 11 (1999) 3355.
[13] M. Born, E. Wolf, in: Principles of Optics, sixth ed., Pergamon, Oxford, 1980, p. 55.
[14] L. Nevot, P. Croce, Rev. Phys. Appl. 15 (1980) 761.
[15] R.W.C. Hausen, J. Wolske, D. Wallace, M. Bissen, NIM A 347 (1994) 249.
[16] T. Takahagi, I. Nagai, A. Ishitani, H. Kuroda, J. Appl. Phys. 64 (1988) 3516.
[17] R.V. Nandedkar, K.J.S. Sawhney, G.S. Lodha, A. Verma, V.K. Raghuvanshi, A.K. Sinha, M.H. Modi, M. Nayak, Curr. Sci. 82 (2002) 298.